# VISUALIZATION OF SOUND FIELD BY MEANS OF SCHLIEREN METHOD WITH SPATIO-TEMPORAL FILTERING

*Nachanant Chitanont, Keita Yaginuma, Kohei Yatabe, Yasuhiro Oikawa*

Department of Intermedia Art and Science, Waseda University, Tokyo, Japan

**ABSTRACT**

Visualization of sound field using Schlieren technique provides many advantages. It enables us to investigate the change of the sound field in real-time from every point of the observing region. However, since the density gradient of air caused by the disturbance of acoustic field is very small, it is difficult to observe the audible sound field from the raw Schlieren video. In this paper, to enhance visibility of the audible sound fields from the Schlieren videos, we propose to use spatio-temporal filters for extracting sound information and for noise removal. We have utilized different filtering techniques such as the FIR bandpass filter, the Gaussian filter, the Wiener filter and the 3D Gabor filter, to do this. The results indicate that the data observed after using these signal processing methods are clearer than the raw Schlieren videos.

***Index Terms*—** Sound field visualization, digital filter, spatio-temporal filtering, Schlieren imaging.

## 1. INTRODUCTION

Sound visualization has gained a lot of popularity in recent years due to its ability to understand physical properties of sound. Microphones are normally used for measuring sound field. Generally, a number of microphones are required to acquire the spatial information of sound field [1, 2]. Laser Doppler vibrometer (LDV) is able to measure sound field projections along a laser path without using any microphone [3, 4]. However, visualization of sound field by using LDV technique needs to scan each point to obtain spatial information that can be applied only to a reproducible sound field.

The Schlieren imaging is a method that enables us to acquire the acoustic properties by investigating the density variation caused by the disturbance of the acoustic field recorded by a high-speed camera. The advantage of the Schlieren method is that it can investigate the change of sound properties in the real-time from every point of field. The Schlieren method was originally developed for visualizing fluid flows [5, 6]. In acoustics, researchers have focused on the visualization of strong ultrasonic sound whose pressure is very large [7, 8, 9]. There are only few researchers have proposed methods to visualize audible sound field [10]. The change in the density gradient of air caused by the disturbance of audible sound field is very small. Therefor, it is difficult to visualize the audible sound field from the raw Schlieren video.

In this paper, we propose to use spatio-temporal filters [11, 12] for extracting sound information and for noise removal. We utilized different filtering techniques such as the FIR bandpass filter, the Gaussian filter, the Wiener filter and the 3D Gabor filter for extracting sound field information to enhance the visualization of the audible sound fields from the Schlieren videos. We used a two-lens Schlieren recording system to record the audible sound field data. We confirm that the propose methods effectively enhance the visibility of the audible sound fields.

## 2. VISUALIZATION OF SOUND FIELD USING SCHLIEREN METHOD

### 2.1. Refraction of light in Schlieren system

Visualizing sound from a Schlieren system is based on refraction of light beams passing through a transparent media whose refractive index varies with positions [13]. For gases, the linear relationship between the refractive index $n$ and the gas density $\rho$, with the Gladstone-Dale constant for air $G$ = $0.23$ cm$^3$/g, is represented as

$$n = G\rho + 1. \tag{1}$$

If light beams travel in the $z$ direction and the length between two lens is $L$, the deflection angles in the $x$ and $y$ direction $\varepsilon_x, \varepsilon_y$ are represented as

$$\varepsilon_x = \frac{L}{n_0}\frac{\partial n}{\partial x}, \quad \varepsilon_y = \frac{L}{n_0}\frac{\partial n}{\partial y}, \tag{2}$$

where $n_0$ is the standard refractive index. By substituting Eq. (1) into Eq. (2), we get the relationship between the deflection angles and the density gradients of air $\partial\rho/\partial x, \partial\rho/\partial y$:

$$\varepsilon_x = \frac{GL}{n_0}\frac{\partial \rho}{\partial x}, \quad \varepsilon_y = \frac{GL}{n_0}\frac{\partial \rho}{\partial y}. \tag{3}$$

Equation (3) indicates that the light beams are refracted due to the variation of the refractive index or the density of air, which is created by the sound field.

978-1-4673-6997-8/15/$31.00 ©2015 IEEE

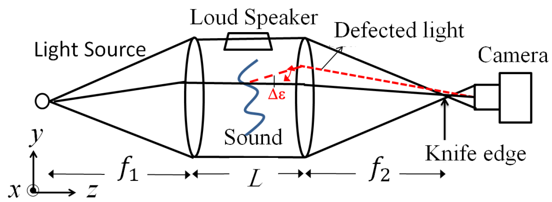


(a)

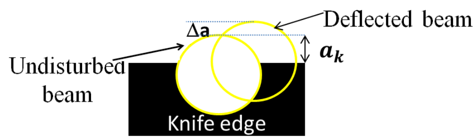


(b)

**Fig. 1**. Drawing of Schlieren system and the displacement of the light beam. (a) two-lens Schlieren system with $f_1$ = 100 cm, $f_2$ = 102 cm and $L$ = 100, (b) horizontal displacement of light beam.

### 2.2. Illumination of Schlieren image by refraction of light

The illumination of a Schlieren image depends on the position of a knife-edge placed in the system. If there are no refractions, the illumination of the background will be formed uniformly. However, in the case of refraction, the image is displaced by a small angle $\varepsilon$ at a corresponding image at a knife-edge as shown in Fig 1 (b). Let $\Delta a$ be the displacement of the light beams

$$\Delta a = \varepsilon f_2, \tag{4}$$

where $f_2$ is the focal length of second lens and $\varepsilon$ is the deflection angle. If the light source is uniformly bright, the contrast $\Delta E/E$ of the Schlieren image is formulated as

$$\frac{\Delta E}{E} = \frac{\Delta a}{a_k}, \tag{5}$$

where $a_k$ is the diameter of the light beam subtracted by the position of the knife-edge. Combining Eq. (4) and Eq. (5) we get

$$\frac{\Delta E}{E} = \frac{\varepsilon f_2}{a}. \tag{6}$$

Equation (6) confirms that we can acquire the deflection angle by analyzing the contrast of the Schlieren image.

### 2.3. Relation between sound and Schlieren video

From the Newtonian equation of motion, the relationship between variation of the particle velocities $\partial v_x/\partial t, \partial v_x/\partial t$ and the gradients of the sound pressure $\partial p/\partial x$, $\partial p/\partial y$ are represented as

$$\frac{\partial v_x}{\partial t} = -\frac{1}{\rho_0}\frac{\partial p}{\partial x}, \quad \frac{\partial v_y}{\partial t} = -\frac{1}{\rho_0}\frac{\partial p}{\partial y}. \tag{7}$$

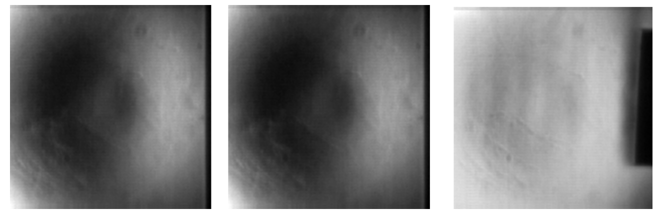

**Fig. 2**. Schlirern images of 10 kHz, 15 kHz and 40 kHz sinusoidal sound fields detected by a high-speed camera.

If the sound pressure $p$ is much smaller than the air pressure, then the sound pressure is represented as:

$$p = K\frac{\rho - \rho_0}{\rho_0}, \tag{8}$$

where $K$ is the bulk modulus and $\rho_0$ is the standard density of air. From Eq. (7) and (8), we can acquire the relationship between variation of the particle velocities and the density gradient as

$$\frac{\partial v_x}{\partial t} = -\frac{K}{\rho_0^2}\frac{\partial \rho}{\partial x}, \quad \frac{\partial v_y}{\partial t} = -\frac{K}{\rho_0^2}\frac{\partial \rho}{\partial y}. \tag{9}$$

If we substitute Eq. (8) and (9) into Eq. (3), the obtained deflection angles are represented as

$$\varepsilon_x = \frac{\rho_0 GL}{n_0 K}\frac{\partial p}{\partial x} = -\frac{\partial v_x}{\partial t}\frac{\rho_0^2 GL}{Kn_0}, \tag{10}$$

$$\varepsilon_y = \frac{\rho_0 GL}{n_0 K}\frac{\partial p}{\partial y} = -\frac{\partial v_y}{\partial t}\frac{\rho_0^2 GL}{Kn_0}. \tag{11}$$

From Eq. (11), it shows that the information of sound can be obtained from the deflection angles of the light beams. As shown in the previous sub section, we are able to acquire the defection angles from the contrast of an image which means that the information of sound can be obtained by the contrast of the Schlieren image.

## 3. SPATIO-TEMPORAL FILTERING FOR SCHLIEREN METHOD

The Schlieren images of 10 kHz, 15 kHz and 40 kHz sinusoidal sound fileds without any processing are shown in Fig 2. As the disturbances in air due to the acoustic fields are not very prominent, it was difficult to observe the audible sound fields from the original Schlieren videos. To extract the audible sound fields from the Schlieren videos, we propose four signal processing methods. They include the FIR bandpass filter for the time direction of the Schlieren videos, the Gaussian filter and the Wiener filter for the spatial direction of the Schlieren videos. In addition, the 3D Gabor filter which is a spatio-temporal filter, that filters both the spatial and the time direction of the Schlieren sound field videos simultaneously. The concepts of these methods are described in this section. The parameters of each method are shown in Table 1.

**Table 1**. Parameters of the proposed methods

| Proposed method | | Parameter |
|---|---|---|
| Spatial directional filtering | Gaussian filter | $\sigma = 10$ |
| | Wiener filter | $N = M = 13$ |
| Time directional filtering | Bandpass filter | order = 200 |
| Spatio-temporal filtering | 3D Gabor filter | $\omega_y = 0, \omega_x, \omega_t$ = frequency of sound $\sigma_x = \sigma_y = \sigma_t = 8$ |

### 3.1. Removing DC component

Firstly, because all the intensity values of the recorded Schlieren video are positive, there are large zero frequency components making the sound field difficult to visualize. Therefore, the DC components of the Schlieren video are removed by evaluating average of each pixel in the time direction and subtracting these average from each pixel.

### 3.2. Time directional filtering

The FIR bandpass filter was designed for filtering out the unwanted frequency components in time direction of the Schlieren video. In this paper, we created a narrow bandpass FIR filter [14] by selecting the center of frequency equal to the frequency of the sound field.

### 3.3. Spatial directional filtering

To eliminate the noise in the spatial direction [15, 16] of Schlieren video, two methods are applied including the Gaussian and the Wiener filter.

#### *3.3.1. Gaussian filter*

The Gaussian filter uses Gaussian function as the impulse response of the system [17]. In this paper, we designed two-dimensional Gaussian filter to process the spatial direction of Schlieren video. The impulse response of the Gaussian filter can be represented as

$$g(x,y) = c \exp\left\{-\frac{x^2+y^2}{2\sigma^2}\right\}, \tag{12}$$

where $\sigma$ is the spread parameter, determining the width of Gaussian, $x$ and $y$ are pixels in the rows and columns of the Schlieren image and $c$ is normalizing constant. The output image $\hat{I}(x,y)$ is calculated by the convolution.

$$\hat{I}(x,y) = \sum_{i=-w/2}^{w/2} \sum_{j=-h/2}^{h/2} I(x+i, y+j) g(x,y), \tag{13}$$

where $w$ and $h$ are the width and the height of the impulse response, respectively and $I(x,y)$ is the input image.

#### *3.3.2. Wiener filter*

The goal of the adaptive Wiener filter is to filter out noise that has corrupted a signal based on statistical approach [18, 19]. It utilizes the local mean $\mu$ and and the variance $\sigma^2$ around the adjacent of an image :

$$\mu = \frac{1}{MN} \sum_{n_1,n_2 \in \eta} I(n_1, n_2), \tag{14}$$

$$\sigma^2 = \frac{1}{MN} \sum_{n_1,n_2 \in \eta} I^2(n_1, n_2) - \mu^2, \tag{15}$$

where $\eta$ is the $N$-by-$M$ local adjacent of each pixel in the Schlieren image. Then, the result of the pixelwise Wiener filter is calculated as

$$\hat{I}(x,y) = \mu + \frac{\sigma^2 - v^2}{\sigma^2}(I(n_1,n_2) - \mu), \tag{16}$$

where $v^2$ is the average of all the local estimated variances.

### 3.4. Spatio-temporal filtering

The 3D-Gabor filter [20] is applied for filtering both the spatial and the time direction of the Schlieren videos simultaneously. According to the one dimensional Gabor filter, it is simply a Gaussian window multiplied by a cosine wave

$$h(t) = \frac{1}{\sqrt{2\pi}\sigma} \exp\left\{\frac{-t^2}{2\sigma^2}\right\} \cos(\omega_0 t). \tag{17}$$

The amplitude spectrum of the Gabor filter $|H(\omega)|$ is the sum of a pair of Gaussian centered at $\omega_0$ and $-\omega_0$ in the frequency domain

$$|H(\omega)| = \frac{1}{2\sqrt{2\pi}} \exp\left\{\frac{-\sigma^2}{2}(\omega - \omega_0)^2\right\}$$
$$\frac{1}{2\sqrt{2\pi}} \exp\left\{\frac{-\sigma^2}{2}(\omega + \omega_0)^2\right\}.$$

From Eq. (18), narrowing the Gaussian window in space-time domain broadens the bandpass window in the spatio-temporal frequency domain and vice versa. Impulse response of 3D Gabor filter is defined as

$$h(x,y,t) = \frac{1}{\sqrt{2\pi^3}\sigma_x\sigma_y\sigma_t} \times \exp\left\{\frac{-x^2}{2\sigma_x^2} + \frac{-y^2}{2\sigma_y^2} + \frac{-t^2}{2\sigma_t^2}\right\}$$
$$\times \cos(\omega_{x_0} x + \omega_{y_0} y + \omega_{t_0} t), \tag{18}$$

where $(\omega_{x_0}, \omega_{y_0}, \omega_{t_0})$ are the center frequencies, and $(\sigma_x, \sigma_y, \sigma_t)$ are the spread parameters of the spatio-temporal Gaussian window.

## 4. EXPERIMENTS AND RESULTS

### 4.1. Experimental set up and recording

Audible sound fields were observed by using a high-speed two-lens Schlieren system as shown in Fig. 1 (a). Sinusoidal

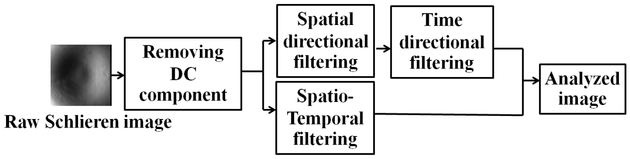


**Fig. 3**. Procedure of visualization of sound field

sound of frequencies 10 kHz and 15 kHz were used to test our methods. We used the YAMAHA MSP-7 STUDIO loudspeaker for testing. The NAC MEMRECAM HX-3 with 96,000 frames per second was used to record $256 \times 256$ pixel Schlieren videos. First, we generated sinusoidal sound waves from the loudspeaker whose interaction with air causes the refraction. We put a knife-edge at the focal point of second lens. The knife-edge blocks the light rays refracted by the sound field, which is finally detected by the high-speed camera.

### 4.2. Experimental Result

We have used different filtering techniques mentioned in the section above. First, we recorded the sound field data by using the Schlieren technique. The DC components were removed for eliminating the large zero frequency components of the Schlieren videos. Then, spatio-temporal filters were used to process the Schlieren data. In our experiment, we provided stationary sinusoidal waves of frequencies 10 kHz and 15 kHz to test our methods. Since there are a lot of noise in the Schlieren images after removing the DC components, we used the spatial filter such as the Gaussian and the Wiener filter to remove noise from the image. Then, the FIR bandpass filter was applied in the time direction to extract the audible sound fields from data. The 3D Gabor filter, on the other hand, is able to process the data in both the spatial and the time direction. The processing procedure of sound field visualization is shown in Fig. 3. Figure 4 and Fig. 5 show the sound fields obtained by our proposed methods. It confirms that temporal filtering is effective for the extraction of information of audible sound fields, and the spatial filtering is effective for noise subtraction.

## 5. CONCLUSION

In order to enable the visualization of the audible sounds field with the Schlieren method, we proposed methods for extracting information of audible sound fields using spatio-temporal filtering. As a result, we confirmed that the temporal filtering is effective for the extraction of the information of audible sound fields, and that the spatial filtering is effective for noise subtraction. However, in this experiment, we visualized only stationary sound fields using spatio-temporal filters for each measured data. In future work, we will use spatio-temporal filter bank which will be visualize a transitional sound field.

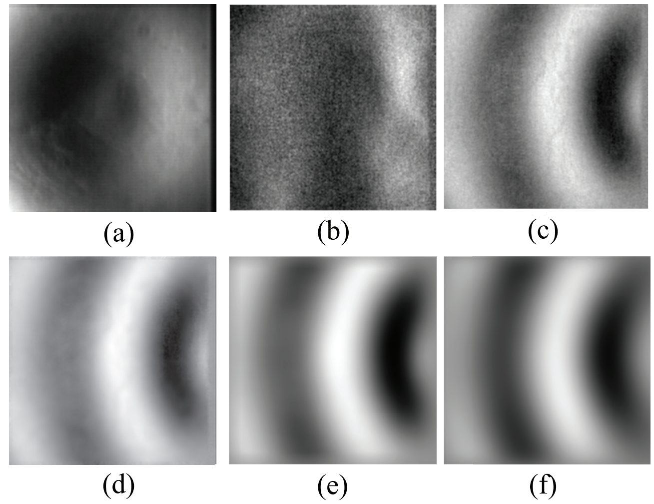


**Fig. 4**. 10 kHz sinusoidal sound field. (a) Measured data, (b) data without DC component, (c) time directional filtering by bandpass filter, (d) spatio-temporal filtering by bandpass and Wiener filter, (e) spatio-temporal filtering by bandpass and Gaussian filter, (f) spatio-temporal filtering by 3D Gabor filter.

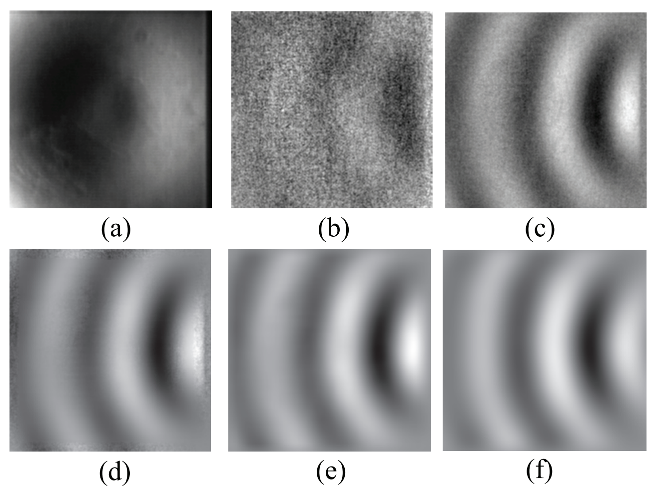


**Fig. 5**. 15 kHz sinusoidal sound field. (a) Measured data, (b) data without DC component, (c) time directional filtering by bandpass filter, (d) spatio-temporal filtering by bandpass and Wiener filter, (e) spatio-temporal filtering by bandpass and Gaussian filter, (f) spatio-temporal filtering by 3D Gabor filter.

In addition, with the Schlieren method, it is possible to measure the integrated value on an optical path of parallel light. However, if we can measure the data of a point or a plane, we can apply this method for recording a 3-dimensional sound field. Thus, we will think about the method to extract the information of the sound field from the measured data and we want to apply this method for recording a 3-dimensional sound field.

## 6. REFERENCES


[1] Y. Yamasaki and T. Itow, "Measurement of spatial information in sound field by closely located four point microphone method," *J. Acoust. Soc. Jpn.(E)*, vol. 10, pp. 101–110, 1989.

[2] K. Endo, T. Horikoshi, Y Yamasaki, and T. Itow, "Grasp and estimation of spatial information in a room by closely locate four point microphone method," 1986, pp. 909–919.

[3] Y. Oikawa, M. Goto, Y. Ikeda, T. Takizawa, and Y. Yamasaki, "Sound field measurement based on reconstruction from laser projections," in *Proc. ICASSP*, 2005, vol. 4, pp. 661–664.

[4] Y. Oikawa, T. Hasegawa, Y. Ouchi, Y. Yamasaki, and Y. Ikeda, "Visualization of sound field and sound source vibration using laser measurement method," in *20th Int. Congr. Acoust. (ICA)*, Aug 2010, vol. 898.

[5] C. Brownlee, V. Pegoraro, S. Shankar, P.S. McCormick, and C. D. Hansen, "Physically-based interactive flow visualization based on schlieren and interferometry experimental techniques," *IEEE Trans. Vis. Comput. Graphics*, vol. 17, no. 11, pp. 1574–1586, Nov. 2011.

[6] D.R. Jonassen, G.S. Settle, and M.D. Tronosky, "Schlieren "PIV" for turbulent flows," *Opt. Laser. Eng.*, vol. 44, no. 3–4, pp. 190–207, 2006.

[7] D. Mller, N. Degen, and J. Dual, "Schlieren visualization of ultrasonic standing waves in mm-sized chambers for ultrasonicparticle manipulationjet flow," *J. Nanobiotechnology.*, vol. 11, no. 21, pp. 1–5, Jun. 2013.

[8] G. Caliano, A.D. Savoia, and A. Iula, "An automatic compact schlieren imaging system for ultrasound transducer testing," *IEEE Trans. Ultrason., Ferroelectr., Freq. Control*, vol. 59, no. 9, pp. 2102–2110, Sep. 2012.

[9] E.K. Reichel, S.C Schneider, and B.G. Zagar, "Characterization of ultrasonic transducers using the schlieren-technique," in *Proc.I2MTC*, May 2005, vol. 3, pp. 1956–1960.

[10] M.J. Hargather, G.S. Settles, and M.J. Madalis, "Schlieren imaging of loud sounds and shock waves in air near the limit of visibility," *ShWav.*, vol. 20, no. 1, pp. 9–17, Feb. 2010.

[11] Y. Sonoda and Y. Nakazono, "Optical flow using spatiotemporal filtering," *Int. J. Comput. Vision.*, vol. 1, pp. 279–320, 1988.

[12] R.V. Arjunan and V.V. Kumar, "Adaptive spatio-temporal filtering for video denoising using integer wavelet transform," in *ICETECT*, 2011, pp. 842–846.

[13] G.S. Sattle, *Schlieren and Shadowgraph Technique*, Springer, 2001.

[14] I.W. Selesnick, M. Lang, and C.S. Burrus, "A modified algorithm for constrained least square design of multiband FIR filters without specified transition bands," *IEEE Trans. Signal Process*, vol. 46, no. 2, pp. 497–501, 1998.

[15] A. Buades, B. Coll, and J.M. Morel, "A review of image denoising algorithms, with a new one," *Multiscale. Model. Simul.*, vol. 4, pp. 490–530, 2005.

[16] A.A. Mahmoud, S.EL. Rabaie, T.E. Taha, O. Zahran, F.E.A. El-Samie, and W. Al-Nauimy, "Comparative study between different denoising filters for speckle noise reduction in ultrasonic bmode images," in *Proc. ICENCO*, 2012, vol. 1, pp. 293–298.

[17] B.K S. Kumar, "Image denoising based on gaussian/bilateral filter and its method noise thresholding," *Signal Image Video Pr.*, vol. 7, no. 6, pp. 1159–1172, 2013.

[18] F. Jin, P. Fieguth, L. Winger, and E. Jernigan, "Adaptive wiener filtering of noisy images and image sequences," in *Proc. ICIP*, 2003, vol. 3, pp. III–349–352.

[19] C. Abe and T. Shimamura, "Iterative edge-preserving adaptive wiener filter for image denoising," *IJCEE*, vol. 4, no. 4, pp. 503–506, Aug. 2012.

[20] Y. Wang and C.S. Chua, "Face recognition from 2d and 3d images using 3d gabor filtersterative edge-preserving adaptive wiener filter for image denoising," *Image. Vision. Comput.*, vol. 23, no. 11, pp. 1018–1028, 2005.